PLASMID DNA REPLICATION AND TOPOLOGY AS VISUALIZED BY TWO-DIMENSIONAL AGAROSE GEL ELECTROPHORESIS

Running title: Plasmid's Replication and Topology

Keywords: DNA Replication / Fork blockage / Supercoiling / Catenation / Knotting / Recombination / *Escherichia coli*

Schvartzman, J.B.*; M.L. Martínez-Robles; P. Hernández and D.B. Krimer

Departamento de Biología Celular y del Desarrollo,
Centro de Investigaciones Biológicas (CSIC), Ramiro de Maeztu 9,
28040 Madrid, **SPAIN**.

* **Corresponding author**:

Jorge B. Schvartzman
Departamento de Biología Celular y del Desarrollo
Centro de Investigaciones Biológicas (CSIC)
Ramiro de Maeztu 9, 28040 Madrid, **SPAIN**

Phone: (34) 91 837-3112 ext. 4232
FAX: (34) 91 536-0432
E-mail: schvartzman@cib.csic.es

2009

Abstract

During the last 20 years, two-dimensional agarose gel electrophoresis combined with other techniques such as Polymerase Chain Reaction, helicase assay and electron microscopy, helped to characterize plasmid DNA replication and topology. Here we describe some of the most important findings that were made using this method including the characterization of unidirectional replication, replication origin interference, DNA breakage at the forks, replication fork blockage, replication knotting, replication fork reversal, the interplay of supercoiling and catenation and other changes in DNA topology that take place as replication progresses.

For the scientific community, one of the landmarks of 1987 was the celebration of the first meeting on Eukaryotic DNA Replication organized by Thomas Kelly and Bruce Stillman at Cold Spring Harbor, New York, USA. Looking backwards, despite many brilliant presentations, this meeting is mostly remembered by the formal debut of a particular technique: two-dimensional (2D) agarose gel electrophoresis to analyze DNA replication intermediates (RIs). Two versions were introduced: Bonita Brewer and Walton Fangman presented the neutral-neutral version (Brewer and Fangman, 1987) while Joel Huberman brought in the neutral-alkaline one (Huberman et al., 1987). In both cases, the most outstanding outcome was the precise mapping of the yeast 2μm plasmid replication origin. Thereafter, both versions were used to map replication origins in a wide variety of biological systems (Brewer and Fangman, 1988; Gahn and Schildkraut, 1989; Linskens and Huberman, 1988; Liu and Botchan, 1990; Schvartzman et al., 1990). Notwithstanding, in some cases the results obtained disagreed with canonical expectations (Delidakis and Kafatos, 1989; Heck and Spradling, 1990; Krysan and Calos, 1991; Linskens and Huberman, 1990a; Linskens and Huberman, 1990b; Vaughn et al., 1990). These apparent discrepancies led us to look for a simple biological system where we could test the technique in a straightforward manner. Taking this in mind we used neutral-neutral 2D gels to analyze the RIs of a bacterial plasmid: pBR322, the replication features of which were very well known at the time (Martín-Parras et al., 1991). Neutral-neutral 2D gels consist in two consecutive

electrophoreses where the second dimension occurs perpendicular to the first. In addition, the conditions employed during the first dimension minimize the effect of molecular shape on electrophoretic mobility whereas this effect is maximized during the second dimension (Brewer and Fangman, 1987; Friedman and Brewer, 1995). In short, neutral-neutral 2D gels reveal how does a linear DNA fragment replicate. The different patterns generated by the RIs corresponding to a specific DNA fragment indicate if it is replicated by a single fork that moves from one end to the other generating a simple-Y pattern, by two forks that move in diverging directions starting at a common site and generating a bubble pattern or by two converging forks that generate a double-Y pattern (Figure 1).

Uni-directional vs. bi-directional replication as visualized in 2D gels

Bolivar and co-workers engineered pBR322 as a cloning vector several years back (Bolívar et al., 1977a; Bolívar et al., 1977b). One of its most outstanding features is that it contains the uni-directional replication origin of the natural ColE1 plasmid. As a consequence, the 2D gel patterns generated by the RIs of pBR322 are expected to differ from the patterns generated by bi-directional replication. pBR322 monomers were linearized with a number of restriction endonucleases that cleaves the plasmid only once at positions distributed 360º around (Figure 2A) and the corresponding RIs were analyzed in 2D gels (Figure 3). The results obtained confirmed the expectations and revealed that when more than 50% of the population of digested RIs has a double-Y appearance (as in the cases where the plasmids were digested with *Sty*I and *Pvu*II), the resulting 2D gel double-Y arc shows a distinct inflection (Khatri et al., 1989; Martín-Parras et al., 1991). This inflection indicates the presence of a stalled fork that corresponds to the origin.

Origin interference

An unexpected observation was the presence of traces of a simple-Y pattern regardless of the restriction endonuclease that was used to linearize the plasmid. A simple-Y pattern indicates that one replication fork moves throughout plasmid-sized molecules all

around (Brewer and Fangman, 1987; Friedman and Brewer, 1995). In other words, it points that neither initiation nor termination of DNA replication occur in all plasmid-sized replicating molecules. To find out an explanation for this apparent paradox, we transfected *E. coli* cells with pure monomeric, dimeric or trimeric forms of the plasmid and examined the 2D gel patterns generated by the corresponding RIs (Martín-Parras et al., 1992). The results obtained confirmed that initiation of DNA replication occurs only once per plasmid regardless of the number of potential origins present. The DNA digested with *Sty*I and *Pvu*II in Figure 3 corresponds to pBR322 dimers. The strength of the simple-Y signal increased significantly in these two cases compared to all the others in the same figure, which derive from monomers. A map corresponding to a dimeric form of pBR322 is shown in Figure 2B. To illustrate the shape of the corresponding RIs as well as the patterns expected a computer simulation application was used (Viguera et al., 2000). As in each dimer a single origin fires per replication round, we used the aforementioned application to show that the element containing the silent origin is replicated passively leading to a simple-Y pattern after digestion (Figure 4). This phenomenon was later coined "origin interference" and was confirmed for circular and linear chromosomes in prokaryotes and eukaryotes as well (Brewer and Fangman, 1987; Brewer and Fangman, 1988; Brewer and Fangman, 1993; Brewer and Fangman, 1994; Dubey et al., 1994; Hernández et al., 1993; Hyrien and Mechali, 1992; Hyrien and Mechali, 1993; Linskens and Huberman, 1988; Little et al., 1993; Liu and Botchan, 1990; Mahbubani et al., 1992; Marahrens and Stillman, 1994; Nawotka and Huberman, 1988; Schvartzman et al., 1990; Schvartzman et al., 1993; Waldeck et al., 1984; Wiesendanger et al., 1994). This notwithstanding, origin interference was shown to fade away as the potential origins lie further and further apart. In other words, for circular molecules containing two potential origins, both origins can fire simultaneously provided the distance between them exceeds 15 kb (Lucas et al., 2000) .

2D gel patterns generated by broken RIs

The high resolution achieved with 2D gels allows the identification of infrequent events that lead to secondary populations, derivative from the original population of RIs. Indeed, breaks in single-strand are unavoidable during the isolation of DNA. Contrary

to the lack of key consequences in the case of linear molecules, this type of breakage has dramatic consequences for RIs, as breaks in single strands tend to occur more often at forked structures containing single-stranded gaps. In such cases breaks in single strands lead to double-stranded breaks that change the mass as well as the shape and consequently the electrophoretic behaviour of the molecules responsible for the classical 2D gel patterns, generating novel patterns. For uni-directional replicating plasmids, secondary 2D gel patterns were readily identified that derived from breaks in single strands at the stalled fork (the origin) as well as at the moving one (the replisome). These secondary patterns originally identified in *E. coli* plasmids (Martín-Parras et al., 1992) were later confirmed for the DNA isolated from mammalian cells (Kalejta and Hamlin, 1996).

Replication fork blockage

In almost all pBR322 multimers the replication origins are co-oriented. Tandem arrangement is indeed the most common organization found in nature for multimeric plasmids as well as for chromosomal repeats (Caburet et al., 2002). The situation is different for pPI21 (Figure 5), the only stable plasmid recovered from *E. coli* cells transformed with a derivative of pSM19035, a Gram-positive broad host range plasmid originally isolated from *Streptococcus pyogenes* (Ceglowski and Alonso, 1994; Ceglowski et al., 1993).

pPI21 contains two long inverted repeats that comprise 80% of the plasmid. Each inverted repeat contains a unidirectional replication origin. In other words, pPI21 contains two unidirectional ColE1 origins that are oriented head-to-head (Figure 5). This peculiar organization prompted us to investigate how does this plasmid replicate in *E. coli* cells. We anticipated that as in all the multimeric forms studied so far, origin interference would tolerate only one replication origin to fire per replication round. This is indeed what the results indicated. Surprisingly, though, we also found that a specific RI containing a single internal bubble accumulated during the replication of pPI21 (Viguera et al., 1996). When a significant number of replication forks stall at a specific site the relative proportion of a particular RI in the population increases. It is usually

referred that this particular RI accumulates and this accumulation generates a distinct signal on top of the usual 2D gel pattern generated by the whole population of RIs (see Figure 6). For the specific RI that accumulated during the replication of pPI21, the internal bubble spanned precisely between both replication origins. In other words, the silent origin act as a barrier for the replication fork initiated at the active origin. Up to then, polar replication fork barriers (RFBs) had been observed only for the termination region in the *E. coli* chromosome (deMassy et al., 1987; Hill et al., 1987), for some *E. coli* plasmids, such as R6K (Horiuchi and Hidaka, 1988; Sista et al., 1989) and for ribosomal DNA repeats (Brewer and Fangman, 1988; Linskens and Huberman, 1988) and the 3' end of tRNAs (Deshpande and Newlon, 1996) in *Saccharomyces cerevisiae*. This was the first time where it was demonstrated that silent ColE1 origins could also act as polar RFBs. It was later shown that the ability of silent ColE1 origins to act as RFBs resides in the RNAII transcript that primes DNA synthesis in this system (Inselburg, 1974; Marians, 1992; Tomizawa et al., 1974) and more specifically, in the failure of the DnaB *E. coli* replication helicase to unwind the RNA 3' end of RNA-DNA hybrids (Santamaría et al., 1998). Curiously, it was later found that the ring-shaped hexamer DnaB by itself couldn't be directly responsible for replication fork stalling, as it is able to accommodate two DNA strands, and possibly RNA-DNA hybrids, through its central channel (Kaplan, 2000; Pomerantz and O'Donnell, 2008). The most likely candidate, hence, is the DNA polymerase, but so far this is still pure speculation. Nevertheless, mapping the initiation and termination sites at the nucleotide level using termination at a Ter/TUS complex as a control, indicated that blockage of replication forks at inversely oriented silent ColE1 origins is not just a pause but permanent, leading to premature termination events (Santamaría et al., 2000).

Replication knots

The accumulation of a specific RI containing an internal bubble also allowed the identification of RIs displaying knots within the replication bubble. This was the first time replication knots formed *in vivo* were characterized (Viguera et al., 1996). Examination of the molecules containing knotted bubbles formed *in vivo* at the electron microscope revealed that most of the nodes of these knots has a positive sign (Sogo et

al., 1999). This observation indicates the putative organization of precatenanes during DNA replication (Postow et al., 1999). Cloning a Ter site at different distances from the unidirectional replication origin allowed the accumulation of RIs that had replicated 25%, 52% and 81% of the size of the plasmid (Figure 7A). Although knotted RIs become outstanding in nicked or linear molecules containing stalled forks, they are visualized also during unconstrained replication (Olavarrieta et al., 2002b). These experiments confirmed that the number and complexity of knotted bubbles rise as a function of bubble size, suggesting that knotting is affected by both precatenane density and bubble size (Figure 7B). pBR18 is a derivative of pBR322 where the tetracycline resistance gene promoter was replaced by the polylinker of pUC18 (Santamaría et al., 2000). As transcription of this gene occurs head-to-head with replication in pBR322, it was thought that DNA topology might be significantly different between pBR322 and pBR18 where no transcription of the tetracycline resistance gene takes place. Curiously, the number and complexity of knotted bubbles are considerably higher in pBR322 suggesting that the accumulation of positive supercoiling ahead of the transcription and replication forks favours knot formation (Olavarrieta et al., 2002a).

The topology of partially replicated plasmids

The observation that head-on collision of transcription and replication favours the formation of DNA knots (Olavarrieta et al., 2002a), prompted the investigation of the topology of these plasmids in 2D gels (Figures 8 and 9). Indeed, different variations of 2D gels had been used extensively to study the supercoiling of circular molecules (Lee et al., 1981; Oppenheim, 1981; Sundin and Varshavsky, 1980; Wang et al., 1983). The Brewer and Fangman neutral/neutral 2D gel technique was also used to analyze the topology of the 2μ plasmid in *S. cerevisiae* (Brewer et al., 1988). Analysis of pBR18 DNA molecules containing replication forks stalled at different positions was performed in 2D gels where the second dimension occurred in the presence of different concentrations of an intercalating agent. These experiments revealed that contrary to the situation observed for unreplicated forms, partially replicated molecules were unable to recover the electrophoretic mobility they have lost when their native negative supercoiling had been eliminated by increasing concentrations of chloroquine or

ethidium bromide (Figure 10). It was later shown that this behaviour is due to the formation of reversed forks (see Figure 9) induced by positive supercoiling (Olavarrieta et al., 2002c). Reversed forks are also called "chicken-foot" structures (Postow et al., 2001).

Replication fork reversal

Although the regression of replication forks was hypothesized years back as a way to impede its collapse (Cox et al., 2000; Higgins et al., 1976) and molecules containing a Holliday-like junction at one of the forks of a replication bubble were visualized by electron microscopy (Viguera et al., 2000), one of the first experimental evidences suggesting its formation *in vivo* was obtained using 2D gels to examine the RIs of yeast cells that had been exposed to DNA damaging agents (Lopes et al., 2001). The interpretation of the results obtained in some of these latter experiments, however, was challenged by the observation that replication fork reversal occurs spontaneously *in vitro* after restriction enzyme digestion but is prevented if the DNA is crosslinked with psoralen before digestion (Fierro-Fernandez et al., 2007a). Moreover, under conditions that favour branch migration, such as exposure to high temperatures, complete extrusion of nascent-nascent duplexes by fork reversal occurs only for nicked RIs while is prevented in covalently closed molecules (Figure 11). Demonstration that the formation of Holliday-like junctions at both forks of a replication bubble creates a topological constrain that prevents the extensive regression of the forks that would be needed to visualize these structures in 2D gels also challenges the occurrence of this phenomenon *in vivo* (Fierro-Fernandez et al., 2007b). Despite the controversy, though, evidence for the occurrence of both *in vivo* and *in vitro* fork reversal was obtained for the phage T4 (Long and Kreuzer, 2008; Long and Kreuzer, 2009).

Supercoiling and Catenation

High-resolution 2D gels together with numerical simulations were also used to better understand the relationship between the DNA negative supercoiling generated by DNA gyrase and the DNA interlinking that results from replication of circular DNA

molecules during the segregation of sister duplexes. With this aim we analyzed bacterial plasmids arising as a result of DNA replication in *E. coli* cells whose topoisomerase IV activity was inhibited (Figure 12). The results obtained indicated that in those catenanes formed *in vivo*, catenation and negative supercoiling compete with each other. In interlinked molecules with high catenation numbers negative supercoiling is greatly limited. However, when interlinking decreases, as required for the segregation of newly replicated sister duplexes, their negative supercoiling increases (Martínez-Robles et al., 2009). This observation indicates that negative supercoiling plays an active role during progressive decatenation of newly replicated DNA molecules *in vivo*.

In summary, the use of 2D gels to analyze intact forms of bacterial plasmids led to the validation of the topological complexity of the different populations that circular DNA adopt *in vivo* (Lucas et al., 2001; Martín-Parras et al., 1998). It also allowed the formulation of a model to account for a topological and dynamic view of the replicon (Schvartzman and Stasiak, 2004).

Acknowledgements

We acknowledge María José Fernández-Nestosa, Marta Fierro-Fernández, Doris Gómez, Virginia López, Estefanía Monturus de Carandini, Leonor Rodríguez, María Rodríguez, María Tenorio, Zaira García and all our former students for their suggestions and support during the course of this study. This work was sustained in part by grants # BIO2005-02224 and BFU2008-00408/BMC to JBS and BFU2007-62670 to PH from the Spanish Ministerio de Ciencia e Innovación.

References

Bolívar, F., et al., 1977a. Origin of replication of pBR345 plasmid DNA. Proceedings of the National Academy of Sciences of the USA 74, 5265-5269.

Bolívar, F., et al., 1977b. Construction and characterization of new cloning vehicles, II. A multipurpose cloning system. Gene 2, 95-113.

Brewer, B. J., Fangman, W. L., 1987. The localization of replication origins on ARS plasmids in S. cerevisiae. Cell 51, 463-471.

Brewer, B. J., Fangman, W. L., 1988. A replication fork barrier at the 3' end of yeast ribosomal RNA genes. Cell 55, 637-643.

Brewer, B. J., Fangman, W. L., 1993. Initiation at closely spaced replication origins in a yeast chromosome. Science 262, 1728-1731.

Brewer, B. J., Fangman, W. L., 1994. Initiation preference at a yeast origin of replication. Proceedings of the National Academy of Sciences of the USA 91, 3418-3422.

Brewer, B. J., et al., 1988. Analysis of replication intermediates by two-dimensional agarose gel electrophoresis. Cancer Cells 6, 229-234.

Caburet, S., et al., 2002. Combing the genome for genomic instability. Trends Biotech 20, 344-350.

Ceglowski, P., Alonso, J. C., 1994. Gene organization of the Streptococcus pyogenes plasmid pDB101: sequence analysis of the orf eta-copS region. Gene 145, 33-39.

Ceglowski, P., et al., 1993. Functional analysis of pSM19035-derived replicons in Bacillus subtilis. FEMS Microbiol Letters 109, 145-150.

Cox, M. M., et al., 2000. The importance of repairing stalled replication forks. Nature 404, 37-41.

Delidakis, C., Kafatos, F. C., 1989. Amplification enhancers and replication origins in the autosomal chrorion gene cluster of *Drosophila*. EMBO Journal 8, 891-901.

deMassy, B., et al., 1987. Inhibition of replication forks exiting the terminus region of the Escherichia coli chromosome occurs at two loci separated by 5 min. Proceedings of the National Academy of Sciences of the USA 84, 1759-1763.

Deshpande, A. M., Newlon, C. S., 1996. DNA replication fork pause sites dependent on transcription. Science 272, 1030-1033.

Dubey, D. D., et al., 1994. Three ARS elements contribute to the ura4 replication origin region in the fission yeast, Schizosaccharomyces pombe. EMBO Journal 13, 3638-3647.

Fierro-Fernandez, M., et al., 2007a. Replication fork reversal occurs spontaneously after digestion but is constrained in supercoiled domains. Journal of Biological Chemistry 282, 18190-6.

Fierro-Fernandez, M., et al., 2007b. Topological locking restrains replication fork reversal. Proceedings of the National Academy of Sciences of the USA 104, 1500-5.

Friedman, K. L., Brewer, B. J., 1995. Analysis of replication intermediates by two-dimensional agarose gel electrophoresis. In: J. L. Campbell, (Ed.), DNA Replication. vol. 262. Academic Press Inc., 525 B Street, Suite 1900, San Diego, CA 92101-4495.

Gahn, T. A., Schildkraut, C. L., 1989. The Epstein-Barr virus origin of plasmid replication, oriP, contains both the initiation and termination sites of DNA replication. Cell 58, 527-535.

Heck, M. M. S., Spradling, A. C., 1990. Multiple replication origins are used during Drosophila chorion gene amplification. Journal of Cell Biology 110, 903-914.

Hernández, P., et al., 1993. Conserved features in the mode of replication of eukaryotic ribosomal RNA genes. EMBO Journal 12, 1475-1485.

Higgins, N. P., et al., 1976. A model for replication repair in mammalian cells. Journal of Molecular Biology 101, 417-425.

Hill, T. M., et al., 1987. The terminus region of the Escherichia coli chromosome contains two separate loci that exhibit polar inhibition of replication. Proceedings of the National Academy of Sciences of the USA 84, 1754-1758.

Horiuchi, T., Hidaka, M., 1988. Core sequence of two separable terminus sites of the R6K plasmid that exhibit polar inhibition of replication is a 20 bp inverted repeat. Cell 54, 515-523.

Huberman, J. A., et al., 1987. The in vivo replication origin of the yeast 2 mm plasmid. Cell 51, 473-481.

Hyrien, O., Mechali, M., 1992. Plasmid Replication in Xenopus Eggs and Egg Extracts - A 2D Gel Electrophoretic Analysis. Nucleic Acids Research 20, 1463-1469.

Hyrien, O., Mechali, M., 1993. Chromosomal replication initiates and terminates at random sequences but at regular intervals in the ribosomal DNA of xenopus early embryos. EMBO Journal 12, 4511-4520.

Inselburg, J., 1974. Replication of Colicin E1 plasmid DNA in minicells from a unique replication initiation site. Proceedings of the National Academy of Sciences of the USA 71, 2256-2259.

Kalejta, R. F., Hamlin, J. L., 1996. Composite patterns in neutral/neutral two-dimensional gels demonstrate inefficient replication origin usage. Molecular and Cellular Biology 16, 4915-4922.

Kaplan, D. L., 2000. The 3 '-tail of a forked-duplex sterically determines whether one or two DNA strands pass through the central channel of a replication-fork helicase. Journal of Molecular Biology 301, 285-299.

Khatri, G. S., et al., 1989. The replication terminator protein of E. coli is a sequence-specific contra-helicase. Cell 59, 667-674.

Krysan, P. J., Calos, M. P., 1991. Replication Initiates At Multiple Locations on an Autonomously Replicating Plasmid in Human Cells. Molecular and Cellular Biology 11, 1464-1472.

Lee, C. H., et al., 1981. Unwinding of double-stranded DNA helix by dihydration. Proceedings of the National Academy of Sciences of the USA 78, 2838-2842.

Linskens, M. H. K., Huberman, J. A., 1988. Organization of replication of ribosomal DNA in Saccharomyces cerevisiae. Molecular and Cellular Biology 8, 4927-4935.

Linskens, M. H. K., Huberman, J. A., 1990a. Ambiguities in results obtained with 2D gel replicon mapping techniques. Nucleic Acids Research 18, 647-652.

Linskens, M. H. K., Huberman, J. A., 1990b. The two faces of eukaryotic DNA replication origins. Cell 62, 845-847.

Little, R. D., et al., 1993. Initiation and termination of DNA replication in human rRNA genes. Molecular and Cellular Biology 13, 6600-6613.

Liu, Y., Botchan, M., 1990. Replication of bovine papillomavirus type-1 DNA initiates within an E2-responsive enhancer element. Journal of Virology 64, 5903-5911.

Long, D. T., Kreuzer, K. N., 2008. Regression supports two mechanisms of fork processing in phage T4. Proceedings of the National Academy of Sciences of the USA 105, 6852-7.

Long, D. T., Kreuzer, K. N., 2009. Fork regression is an active helicase-driven pathway in bacteriophage T4. EMBO Reports 10, 394-9.

Lopes, M., et al., 2001. The DNA replication checkpoint response stabilizes stalled replication forks. Nature 412, 557-561.

Lucas, I., et al., 2000. Mechanisms ensuring rapid and complete DNA replication despite random initiation in Xenopus early embryos. Journal of Molecular Biology 296, 769-786.

Lucas, I., et al., 2001. Topoisomerase II can unlink replicating DNA by precatenane removal. EMBO Journal. 20, 6509-6519.

Mahbubani, H. M., et al., 1992. DNA Replication Initiates at Multiple Sites on Plasmid DNA in Xenopus Egg Extracts. Nucleic Acids Research 20, 1457-1462.

Marahrens, Y., Stillman, B., 1994. Replicator dominance in a eukaryotic chromosome. EMBO Journal 13, 3395-3400.

Marians, K. J., 1992. Prokaryotic DNA replication. Annual Review of Biochemistry 61, 673-719.

Martín-Parras, L., et al., 1991. Unidirectional replication as visualized by two-dimensional agarose gel electrophoresis. Journal of Molecular Biology 220, 843-853.

Martín-Parras, L., et al., 1992. Initiation of DNA replication in ColE1 plasmids containing multiple potential origins of replication. Journal of Biological Chemistry 267, 22496-22505.

Martín-Parras, L., et al., 1998. Topological complexity of different populations of pBR322 as visualized by two-dimensional agarose gel electrophoresis. Nucleic Acids Research 26, 3424-3432.

Martínez-Robles, M. L. et al., 2009. Interplay of DNA supercoiling and catenation during the segregation of sister duplexes. Nucleic Acids Research 37, 5126-5137.

Nawotka, K. A., Huberman, J. A., 1988. Two-dimensional gel electrophoretic method of mapping DNA replicons. Molecular and Cellular Biology 8, 1408-1413.

Olavarrieta, L., et al., 2002a. DNA knotting caused by head-on collision of transcription and replication. Journal of Molecular Biology 322, 1-6.

Olavarrieta, L., et al., 2002b. Knotting dynamics during DNA replication. Molecular Microbiology 46, 699-707.

Olavarrieta, L., et al., 2002c. Supercoiling, knotting and replication fork reversal in partially replicated plasmids. Nucleic Acids Research 30, 656-666.

Oppenheim, A., 1981. Separation of closed circular DNA from linear DNA by electrophoresis in two dimensions in agarose gels. Nucleic Acids Research 9, 6805-12.

Pomerantz, R. T., O'Donnell, M., 2008. The replisome uses mRNA as a primer after colliding with RNA polymerase. Nature 456, 762-6.

Postow, L., et al., 1999. Knot what we thought before: the twisted story of replication. Bioessays 21, 805-808.

Postow, L., et al., 2001. Positive torsional strain causes the formation of a four-way junction at replication forks. Journal of Biological Chemistry 276, 2790-2796.

Sánchez-Gorostiaga, A. et al., 2004. Transcription terminator factor reb1p causes two replication fork barriers at its cognate sites in fission yeast rDNA in vivo. Molecular and Cellular Biology 24, 398-406.

Santamaría, D., et al., 1998. DnaB helicase is unable to dissociate RNA-DNA hybrids - Its implication in the polar pausing of replication forks at ColE1 origins. Journal of Biological Chemistry 273, 33386-33396.

Santamaría, D., et al., 2000. Premature termination of DNA replication in plasmids carrying two inversely oriented ColE1 origins. Journal of Molecular Biology 300, 75-82.

Schvartzman, J. B., et al., 1990. Evidence that replication initiates at only some of the potential origins in each oligomeric form of Bovine Papillomavirus Type 1 DNA. Molecular and Cellular Biology 10, 3078-3086.

Schvartzman, J. B., et al., 1993. The migration behaviour of DNA replicative intermediates containing an internal bubble analyzed by 2-dimensional agarose gel electrophoresis. Nucleic Acids Research 21, 5474-5479.

Schvartzman, J. B., Stasiak, A., 2004. A topological view of the replicon. EMBO Reports 5, 256-261.

Sista, P. R., et al., 1989. A host-encoded DNA-binding protein promotes termination of plasmid replication at a sequence-specific replication terminus. Proceedings of the National Academy of Sciences of the USA 86, 3026-3030.

Sogo, J. M., et al., 1999. Formation of knots in partially replicated DNA molecules. Journal of Molecular Biology 286, 637-643.

Sundin, O., Varshavsky, A., 1980. Terminal stages of SV40 DNA replication proceed via multiply intertwined catenated dimers. Cell 21, 103-114.

Tomizawa, J., et al., 1974. Replication of colicin E1 plasmid DNA in cell extracts Origin and direction of replication. Proceedings of the National Academy of Sciences of the USA 71, 2260-2264.

Vaughn, J. P., et al., 1990. Replication initiates in a broad zone in the amplified CHO dihydrofolate reductase domain. Cell 61, 1075-1087.

Viguera, E., et al., 1996. The ColE1 unidirectional origin acts as a polar replication fork pausing site. Journal of Biological Chemistry 271, 22414-22421.

Viguera, E., et al., 2000. Visualisation of plasmid replication intermediates containing reversed forks. Nucleic Acids Research 28, 498-503.

Waldeck, W., et al., 1984. Origin of replication in episomal bovine papilloma virus type 1 DNA isolated from transformed cells. EMBO Journal 3, 2173-2178.

Wang, J. C., et al., 1983. DNA supercoiling and its effects on DNA structure and function. Cold Spring Harbor Symposium on Quantitative Biology 47 Pt 1, 85-91.

Wiesendanger, B., et al., 1994. Replication fork barriers in the xenopus rDNA. Nucleic Acids Research 22, 5038-5046.

Legend to Figures

Figure 1: Cartoon illustrating the shape of the molecules and the different 2D gel patterns generated by bidirectional replication. Non-replicating linear molecules of different sizes are depicted in black; Non-replicating X-shaped recombinants are depicted in blue; RIs containing an internal bubble are depicted in red; RIs generated by two converging forks are called double-Ys and are depicted in fuchsia. Finally, RIs generated by a single fork moving from one end to the other are called simple-Ys and are depicted in green.

Figure 2: Genetic maps corresponding to a monomer (A) and a dimer (B) of the bacterial plasmid pBR322 showing their most prominent features: the unidirectional ColE1 origin, the location and orientation of rop and the ampicillin and tetracyclin resistance genes as well as the location of a number of restriction sites. Note that in the dimer all the elements are co-oriented.

Figure 3: Replication of pBR322 as visualized in 2D gels. Plasmid DNA was isolated from exponentially growing bacteria, digested with the indicated restriction endonuclease (see the maps in Figure 2) and analyzed in 2D gels. The shapes of the corresponding RIs after digestion are shown to the left and were generated with the 2D Gel application (Viguera et al., 2000). The autoradiograms are in the middle and cartoons with the corresponding interpretations are shown to the right. The DNA digested with *Alw*NI, *Pvu*I and *Eco*VI was isolated from cells transformed with monomeric forms of the plasmid whereas the DNA digested with *Sty*I and *Pvu*II was isolated from cells transformed with dimeric forms of pBR322. In the cartoons RIs containing an internal bubble are depicted as solid red lines; Double-Ys as solid fuchsia lines; Non-replicating linears as solid black lines; X-shaped recombinants as dashed blue lines and simple-Ys are depicted as dashed green lines.

Figure 4: 2D gel pattern generated after digestion with *Pvu*II of the dimeric form of pBR322 where a single origin fires per replication round. The shapes of the RIs generated by the element containing the active origin is shown to the left and those

generated by the element containing the inactive origin is shown in the middle. The expected patterns are shown to the right. All figures were generated with the 2D Gel application (Viguera et al., 2000). Compare these expected patterns with those observed in the autoradiogram shown in Figure 3 and note in the latter the presence of a mixture of simple- and double-Ys.

Figure 5: Genetic map of the bacterial plasmid pPI21 showing its most prominent feature: the symmetrical location of two unidirectional ColE1 origins in opposite orientations. Thin lines indicate inverted repeats whereas thick lines indicate unique DNA sequences.

Figure 6: Detection of replication fork barriers (RFBs) in 2D gels. Autoradiograms of linear molecules replicated by one fork moving from one end to the other. The simple-Y pattern generated is decorated by a prominent spot only in (B). This spot indicates that during replication a particular RI accumulates in (B) but not in (A). The autoradiogram corresponds to a minichromosome containing an RFB from the fission yeast *Schizosaccharomyces pombe* ribosomal DNA (Sánchez-Gorostiaga et al., 2004). This observation confirmed that most RFBs are polar and stall replication forks only in one orientation. The autoradiograms are shown to the left and cartoons with their corresponding interpretations are depicted to the right.

Figure 7: Detection of knotted bubbles in 2D gels. (A) Genetic maps of the bacterial plasmids pTerE25, pTerE52 and pTerE81 showing the relative position of their most relevant features are shown on top. Note that unidirectional replication forks initiated at the ColE1 origins are expected to stall when they meet the TerE RFB. This stalling leads to the accumulation of RIs containing an internal bubble with a mass 1.25x, 1.52x and 1.81x the mass of unreplicated plasmids, respectively. (B) 2D gel autoradiogram corresponding to a mixture of RIs of these three plasmids after digestion with a restriction endonuclease that cuts the plasmids only once and outside the bubble with an interpretative cartoon to the right. The arcs formed by discrete spots that appear to the right of the accumulated signals and extend downwards are clearly observed in all cases. These arcs correspond to linear molecules containing an internal bubble where

the two sister duplexes show increasing degrees of knotting (for details see Olavarrieta et al., 2002).

Figure 8: Schematic representations of relaxed (OC) and negatively as well as positively supercoiled (CCC) circular DNA molecules.

Figure 9: Autoradiograms of 2D gels corresponding to pBR18-TerE@StyI where the second dimension occurred without (far left) or in the presence of different concentrations of chloroquine (concentrations in μg/ml are indicated on top). All the autoradiograms were aligned so that the positions of Open Circles (OCs) and Open Replication Intermediates (OCRIs), the electrophoretic mobility of which are not affected by drug concentration, coincided. The positions of CCCs and CCRIs are indicated only in the autoradiogram corresponding to the untreated panel (far left). Note that CCRIs were unable to recover electrophoretic mobility once their native negative supercoiling has been removed.

Figure 10: Schematic representations of negatively and positively supercoiled as well as precatenated (CCCRI) partially replicated circular DNA molecules. A relaxed RI containing reversed forks is shown to the right. Parental strands are depicted in green and blue while nascent strands are depicted in red.

Figure 11: **Exposure of undigested partially replicated plasmids to 65 °C in the presence of 0. 1 M NaCl enhances branch migration and leads to total extrusion of the nascent-nascent duplex but only for nicked forms.** Autoradiograms of 2D gels corresponding to pBR18-TerE@AatII where the second dimension occurred without intercalating agents. For the autoradiogram shown to the *right*, the agarose lane of the first dimension (*1st dim*) containing the DNA sample was incubated at 65 °C with 0.1 M NaCl in TNE for 4 h before proceeding with the second dimension. A diagrammatic interpretation is shown to the *right* of each autoradiogram. The signals resulting from total extrusion of the nascent-nascent duplex are depicted in *gray* and indicated by *arrows*. The *dotted lines* indicate the relative position of open circles (OCs) and nicked RIs (OCRIs) after the first and second dimensions. CCCs, covalently close circles; L,

linears.

Figure 12: Schematic representation of negatively supercoiled and catenated sister duplexes. Parental strands are depicted in green and blue while nascent strands are depicted in red. Solid spots indicate intramolecular nodes whereas asterisks depict intermolecular nodes.

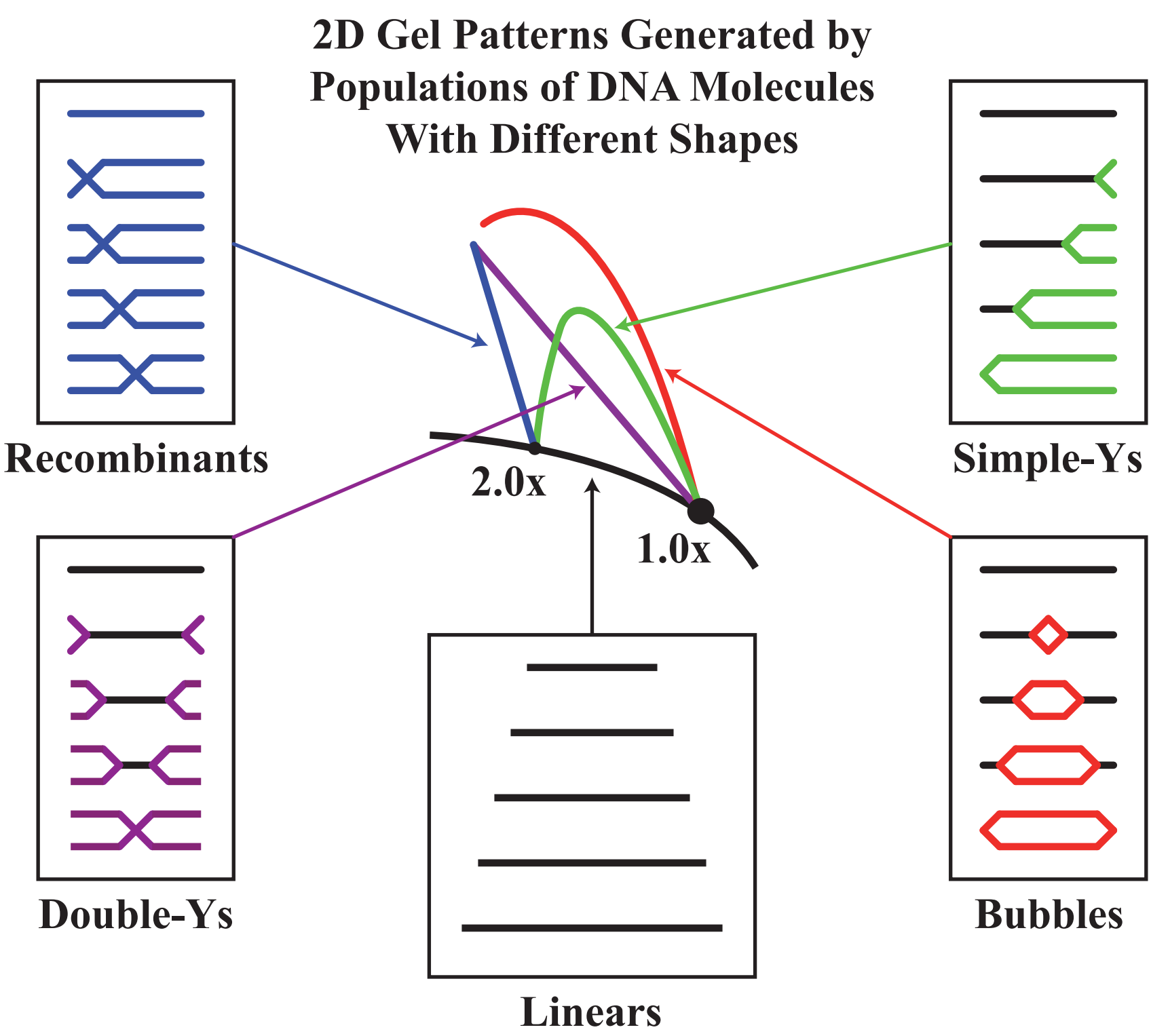
2D Gel Patterns Generated by
Populations of DNA Molecules
With Different Shapes
Recombinants
Simple-Ys
2.0x
1.0x
Double-Ys
Bubbles
Linears

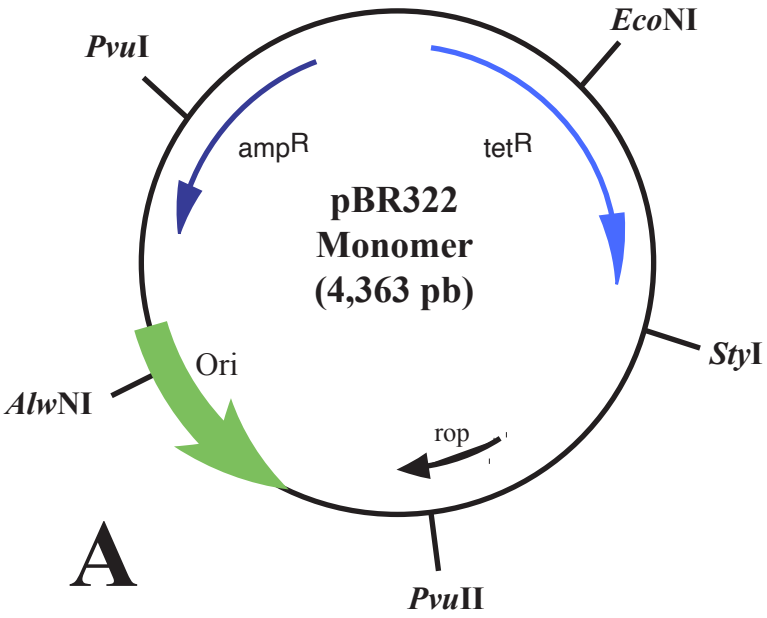
PvuI
EcoNI
ampR
tetR
pBR322
Monomer
(4,363 pb)
StyI
Ori
AlwNI
rop
PvuII

A

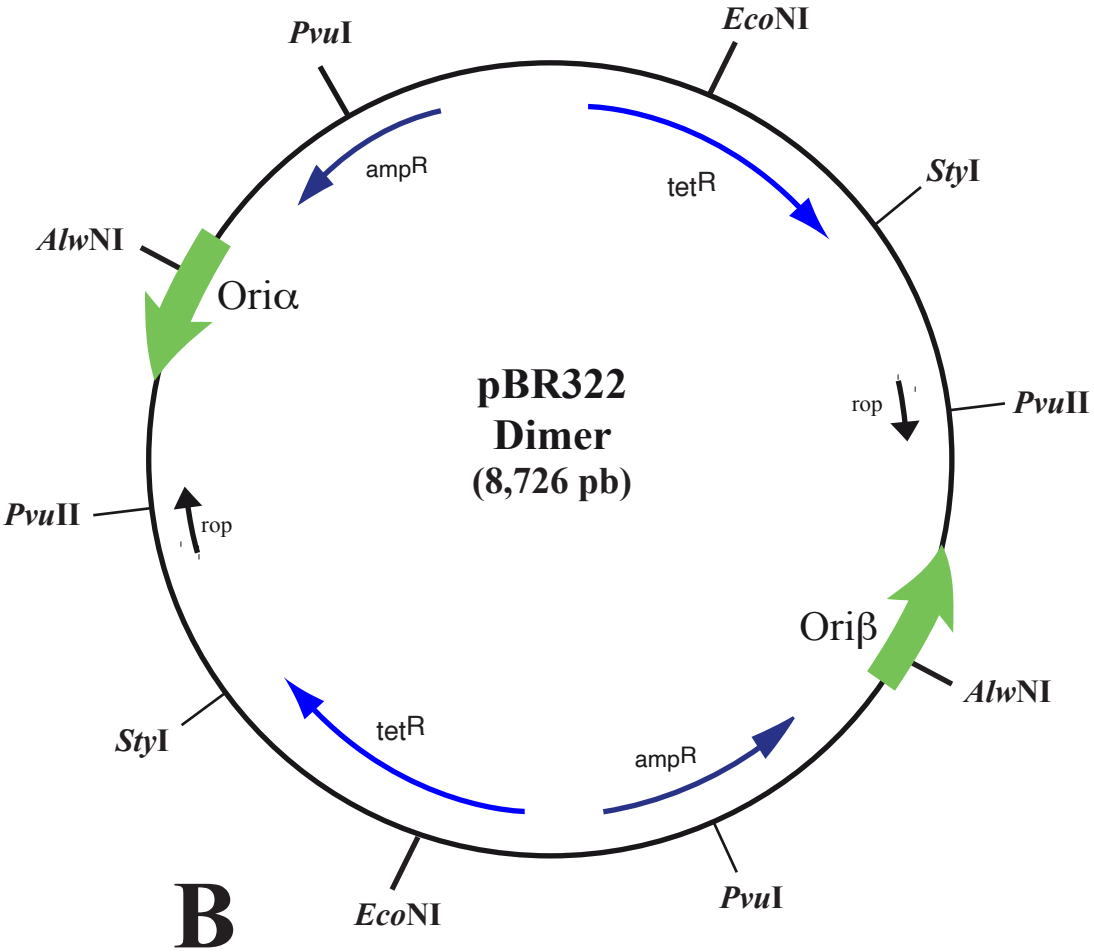
PvuI
EcoNI
ampR
tetR
StyI
AlwNI
Oriα
pBR322
Dimer
(8,726 pb)
rop
PvuII
PvuII
rop
Oriβ
AlwNI
StyI
tetR
ampR
EcoNI
PvuI

B

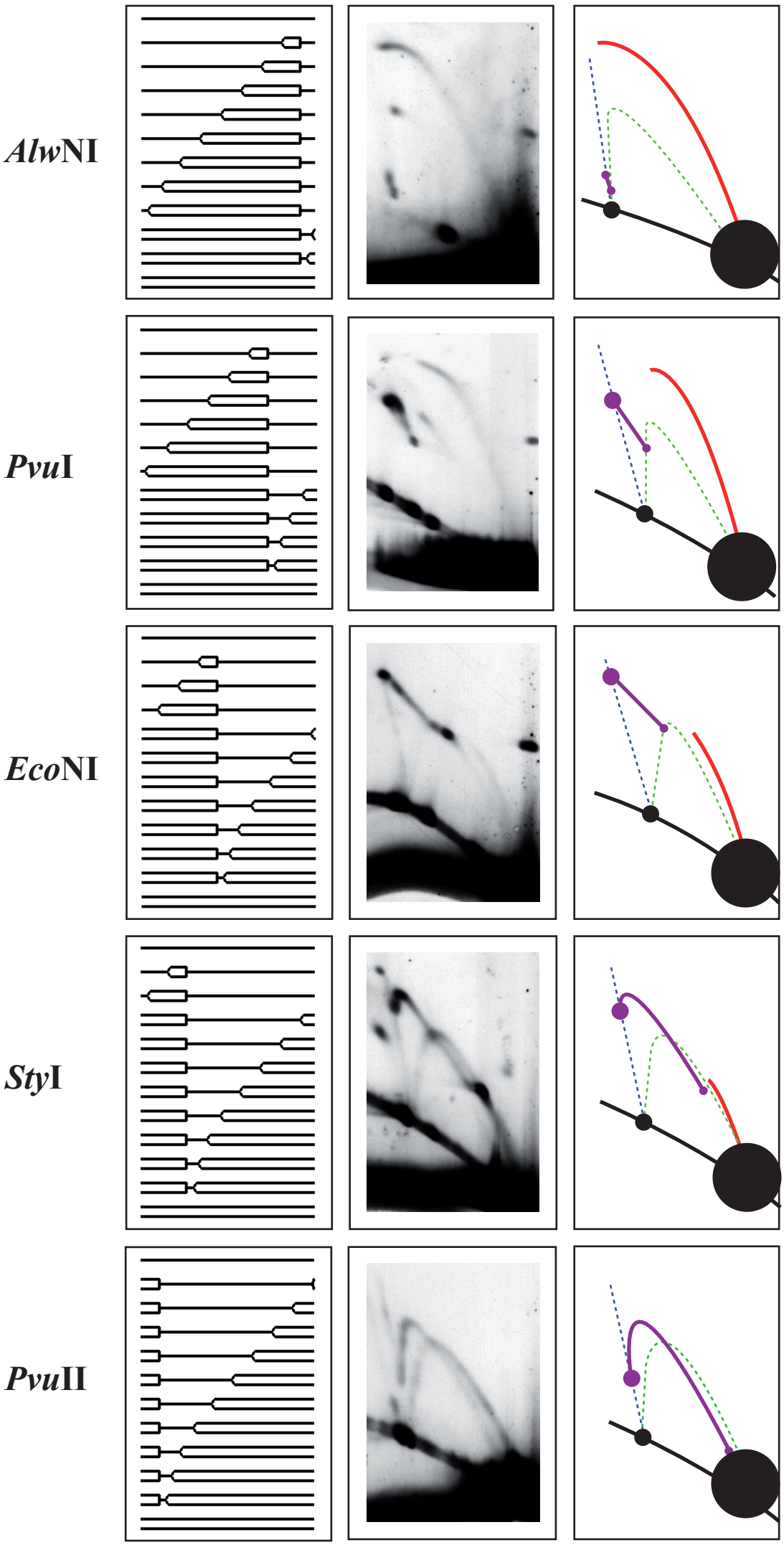
*Alw*NI
*Pvu*I
*Eco*NI
*Sty*I
*Pvu*II

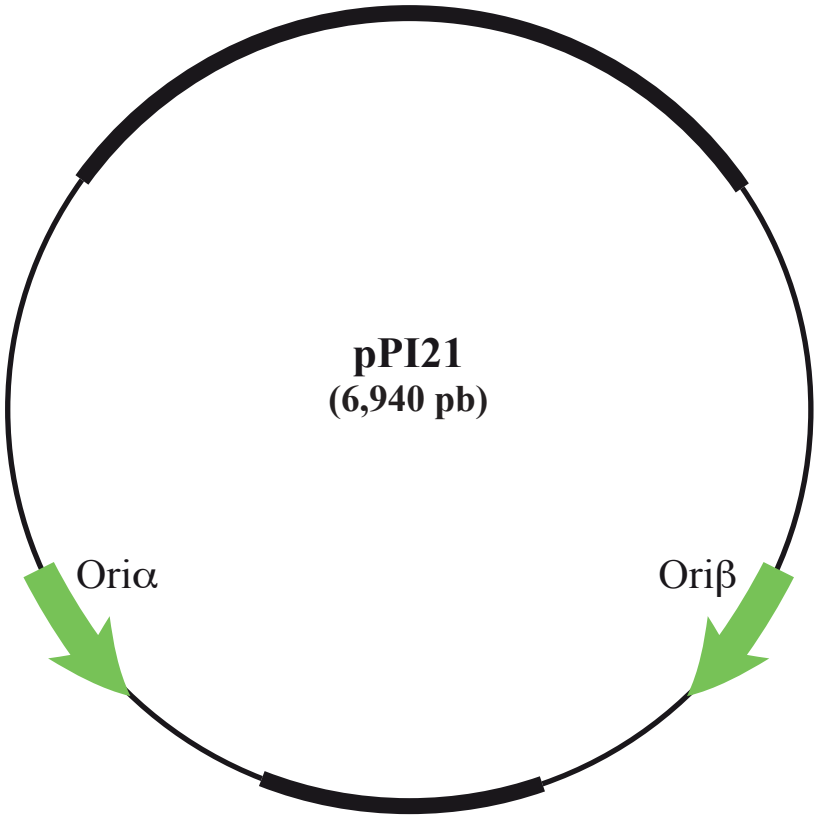
pPI21
(6,940 pb)
Oriα
Oriβ

***Pvu*II**

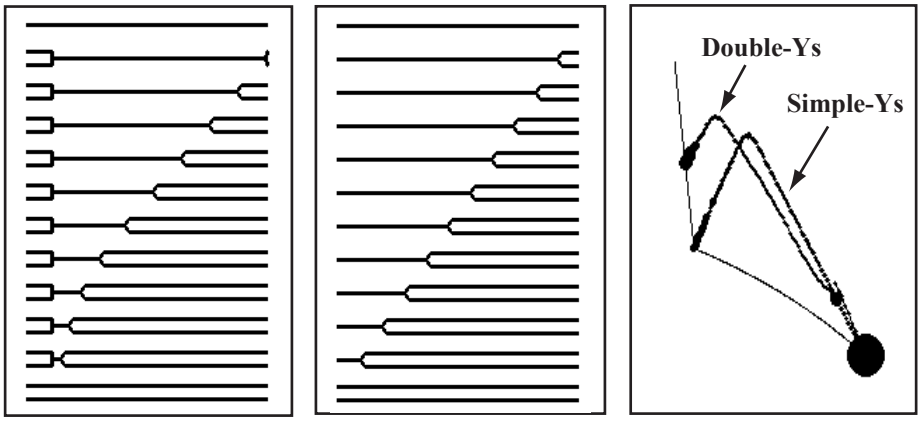

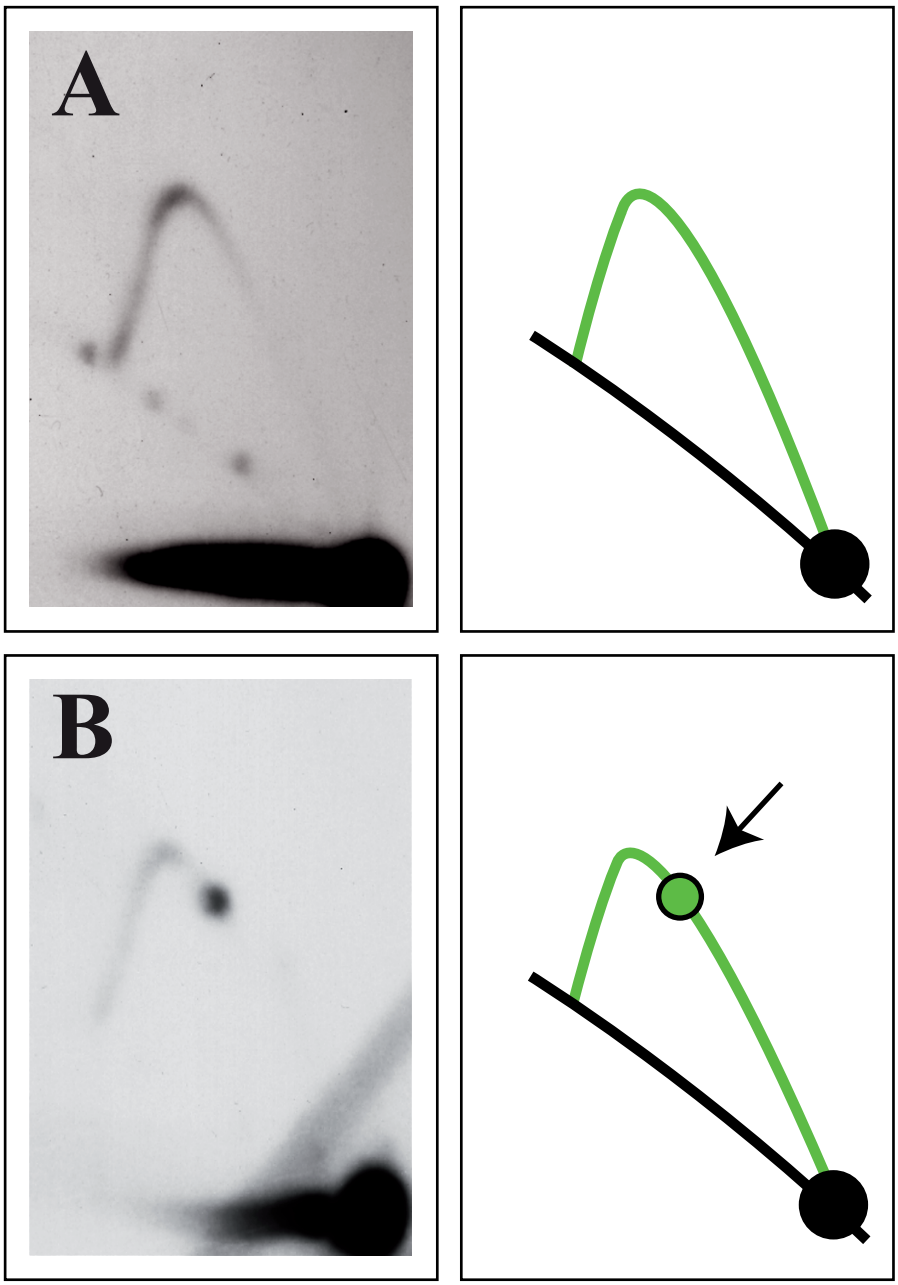
A
B

A

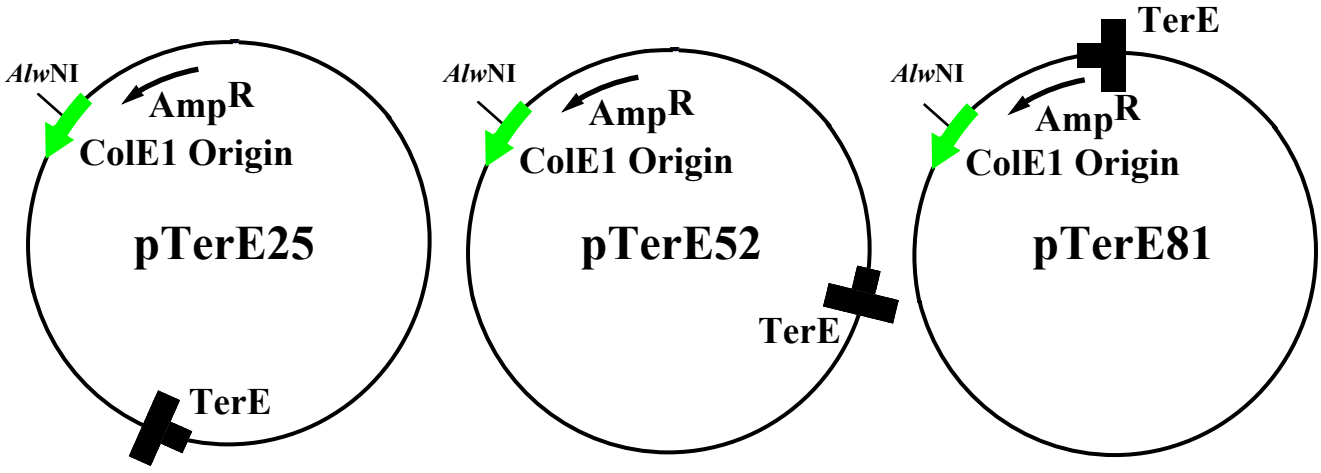
AlwNI
AmpR
ColE1 Origin
pTerE25
TerE
AlwNI
AmpR
ColE1 Origin
pTerE52
TerE
TerE
AlwNI
AmpR
ColE1 Origin
pTerE81

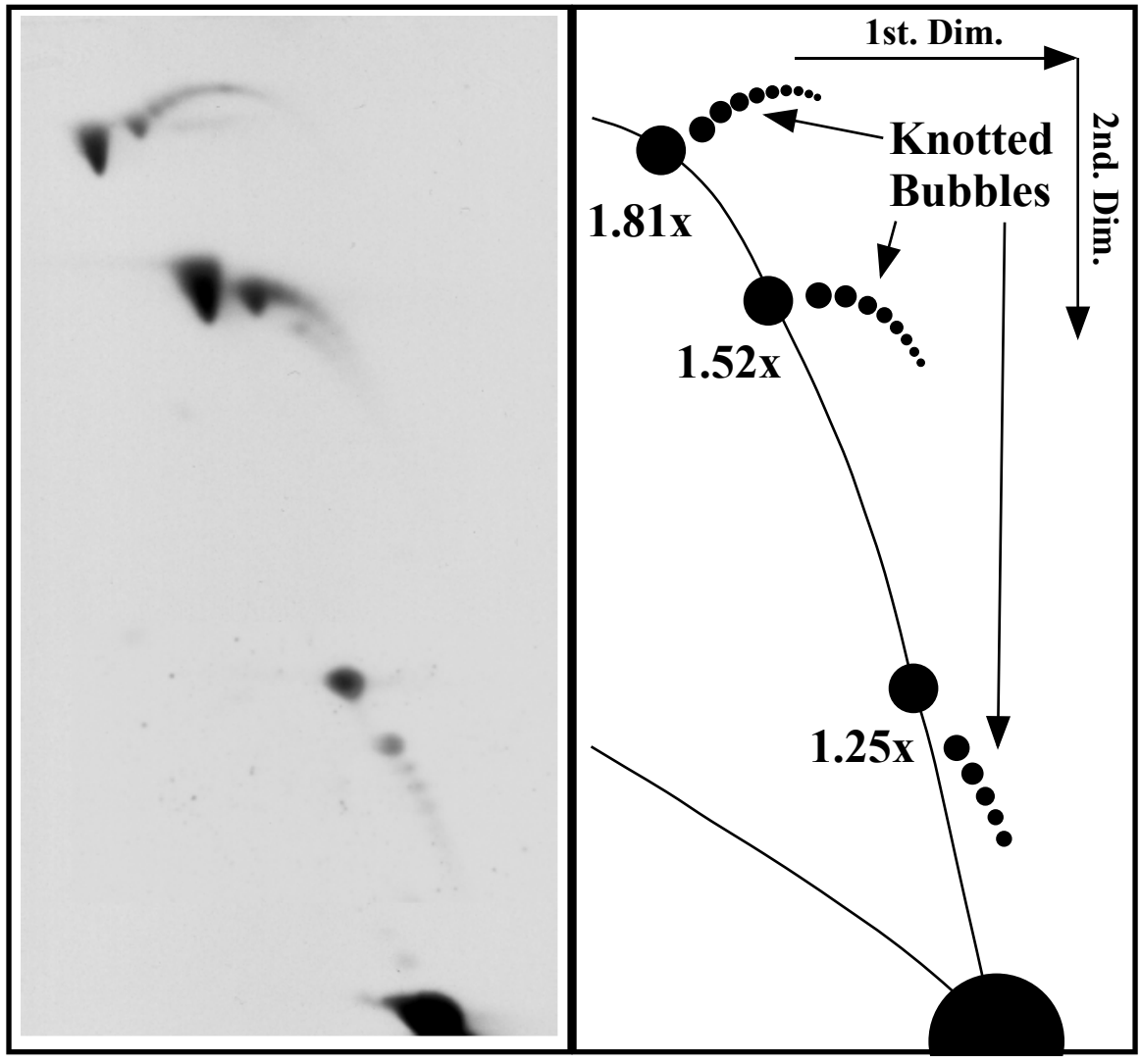
1st. Dim.
2nd. Dim.
Knotted
Bubbles
1.81x
1.52x
1.25x

B

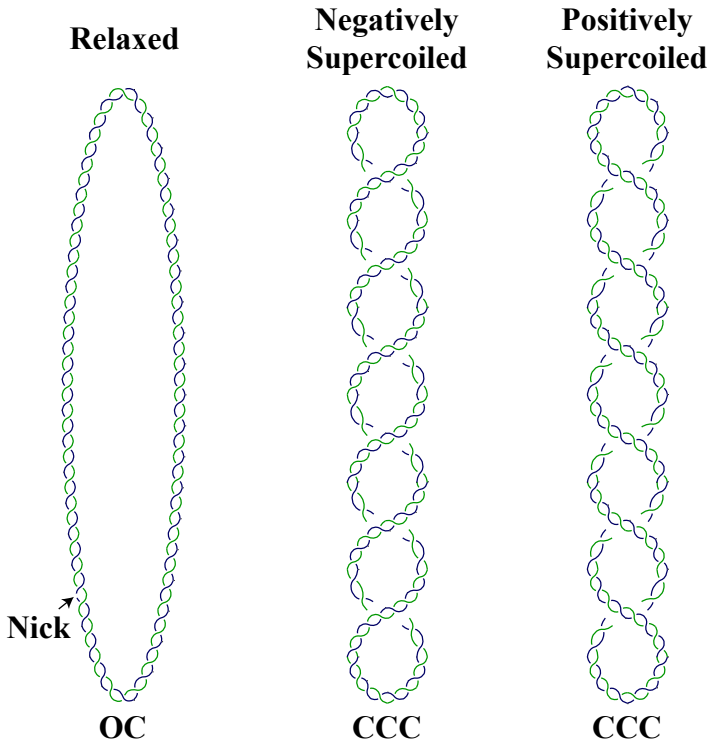
Relaxed
Negatively Supercoiled
Positively Supercoiled
Nick
OC
CCC
CCC

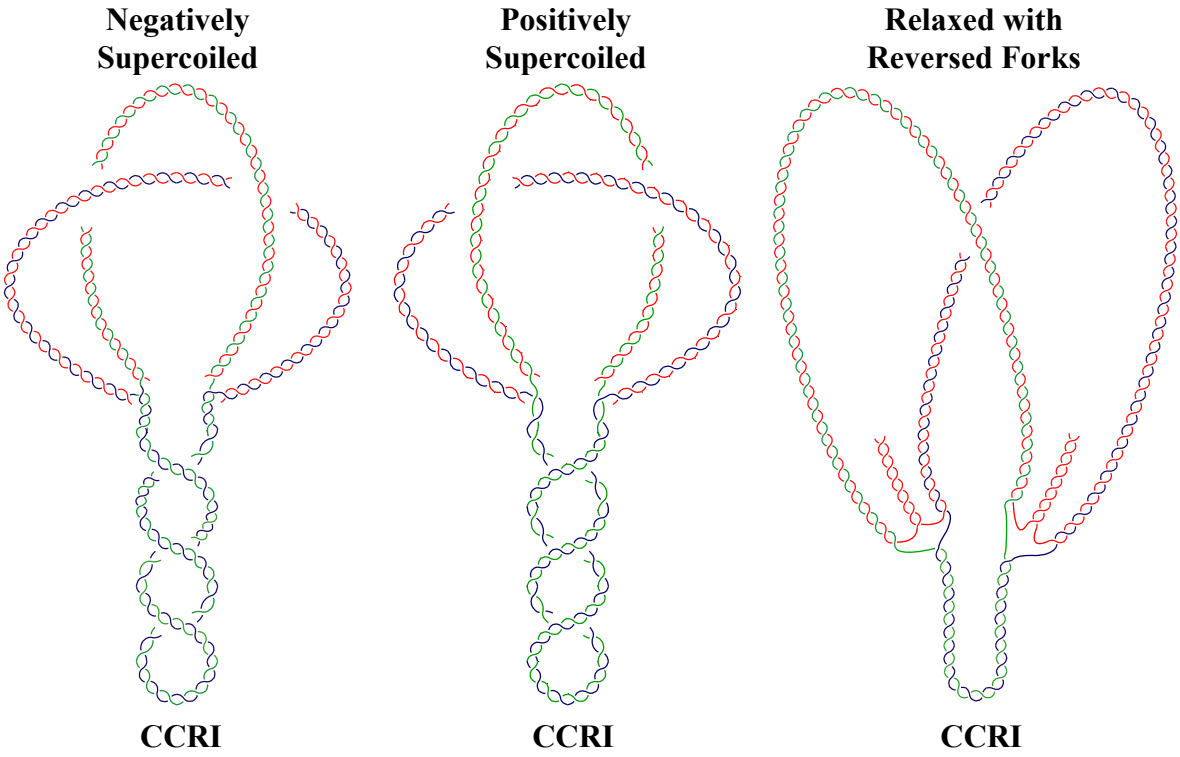
Negatively Supercoiled
Positively Supercoiled
Relaxed with Reversed Forks
CCRI
CCRI
CCRI

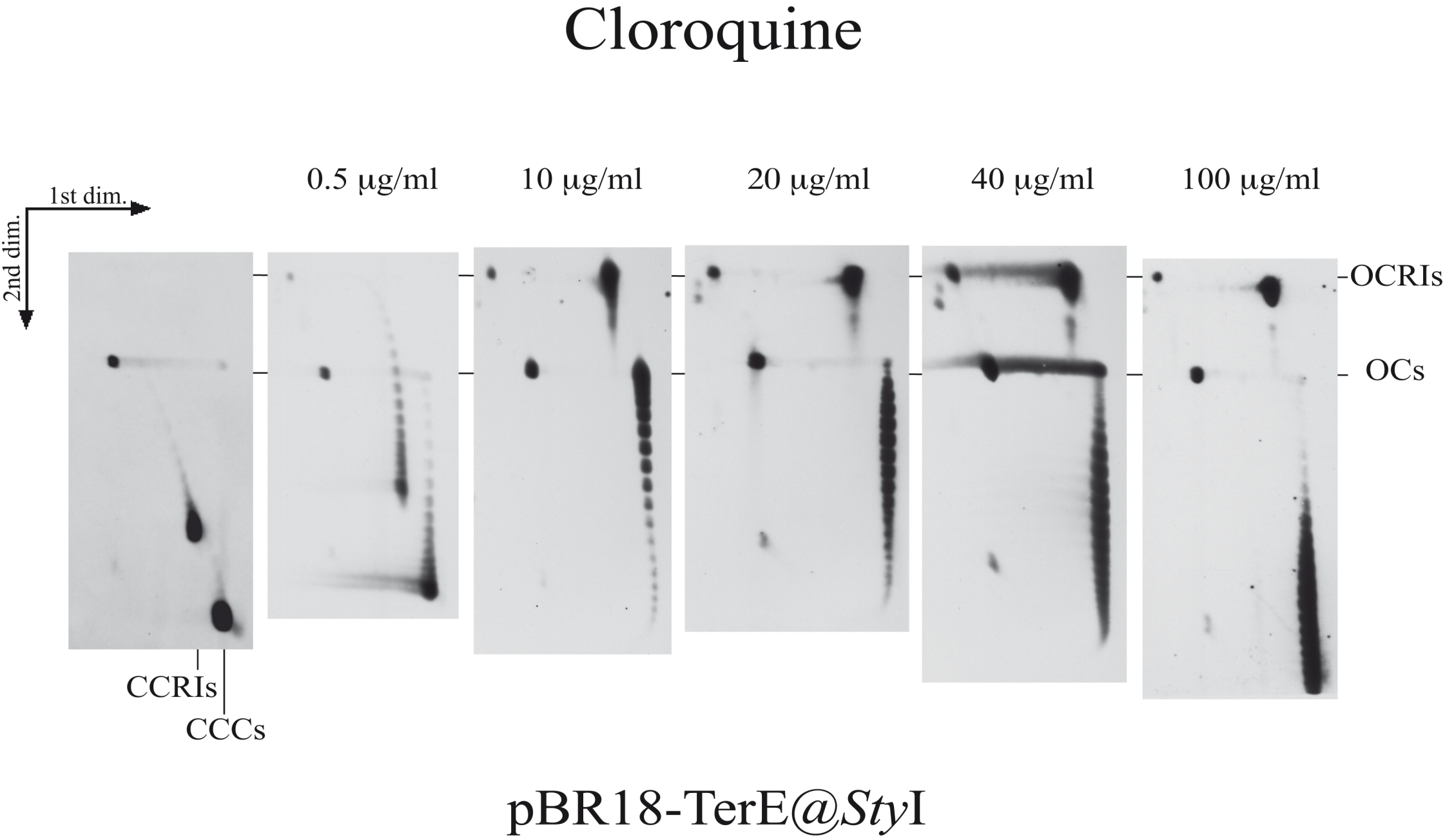
Cloroquine
0.5 µg/ml
10 µg/ml
20 µg/ml
40 µg/ml
100 µg/ml
1st dim.
2nd dim.
OCRIs
OCs
CCRIs
CCCs
pBR18-TerE@StyI

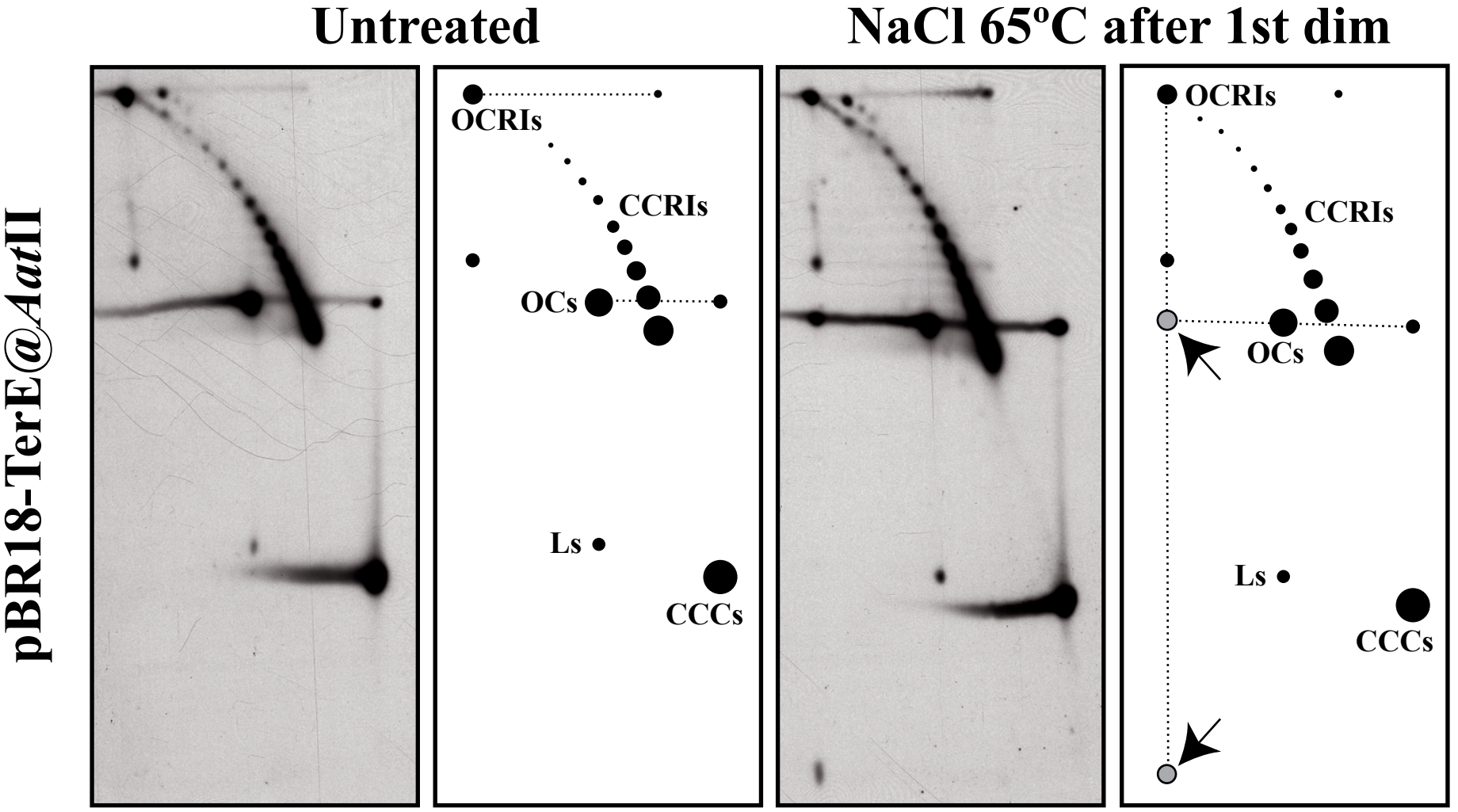
Untreated
NaCl 65ºC after 1st dim
pBR18-TerE@AatII
OCRIs
CCRIs
OCs
Ls
CCCs
OCRIs
CCRIs
OCs
Ls
CCCs